

Optimization of the preparation process of vinblastine sulfate (VBLS)-loaded folate-conjugated bovine serum albumin (BSA) nanoparticles for tumor-targeted drug delivery using response surface methodology (RSM)

Yuangang Zu
Yu Zhang
Xiuhua Zhao
Qi Zhang
Yang Liu
Ru Jiang

Key Laboratory of Forest Plant Ecology, Northeast Forestry University, Ministry of Education, Harbin, Heilongjiang, China

Abstract: Response surface methodology (RSM) was used to optimize the process of preparing bovine serum albumin (BSA) nanoparticles by desolvation, then the resulting BSA nanoparticles (BSANPs) were conjugated with folate to produce a drug carrier system that can specifically target tumors. The anticancer drug, vinblastine sulfate (VBLS), was loaded to this tumor-specific drug carrier system for the purpose of overcoming the nonspecific targeting characteristics and side effects of the drug. A central composite design was applied for modeling the process, which was composed of four independent variables, namely BSA concentration, the rate of adding ethanol (ethanol rate), ethanol amount, and the degree of crosslinking. The mean particle size and residual amino groups of the BSANPs were chosen as response variables. The interactive effects of the four independent variables on the response variables were studied. The characteristics of the nanoparticles; such as amount of folate conjugation, drug entrapment efficiency, drug-loading efficiency, surface morphology and release kinetics *in vitro* were investigated. Optimum conditions for preparing desired BSANPs, with a mean particle size of 156.6 nm and residual amino groups of 668.973 nM/mg, were obtained. The resulting folate-conjugated BSANPs (FA-BSANPs) showed a drug entrapment efficiency of 84.83% and drug-loading efficiency of 42.37%, respectively, and the amount of folate conjugation was 383.996 $\mu\text{M/g}$ BSANPs. The results of this study indicate that using FA-BSANPs as a drug carrier system could be effective in targeting VBLS-sensitive tumors in the future.

Keywords: bovine serum albumin, vinblastine sulfate, folate, targeted drug delivery, nanoparticles, response surface methodology

Introduction

Even with the biological and pharmaceutical advancement that the scientific community has achieved, cancer is still, without doubt, one of the biggest killers worldwide. Vinca alkaloids, camptothecin, and paclitaxel are three kinds of the most commonly used plant derived chemotherapy agents.¹ The four vinca alkaloids, namely vinblastine, vincristine, vindesine, and vinorelbine, are cell cycle specific mitotic inhibitors by binding to the microtubular proteins of the mitotic spindle, causing mitotic arrest and cell death. The four only differ in their antitumor spectra and toxicities.² Vinblastine has poor aqueous solubility and serious side effects, however its transformation to a sulfate (vinblastine sulfate [VBLS]) has, to some extent, overcome its hydrophobicity. However, the systemic administration of VBLS is compromised by severe dose-limiting toxicity

Correspondence: Yuangang Zu
Key Laboratory of Forest Plant Ecology,
Northeast Forestry University,
Ministry of Education, Harbin,
Heilongjiang 150040, China
Tel +86 451 8219 1517
Fax +86 451 8210 2082
Email zygorl@yahoo.com.cn

leading to such side effects as leucopenia and anemia.³ This is not only due to the characteristics of VBLS itself, but more to the nonspecific targeting method of administering the drug which damages both cancer cells and healthy noncancerous tissues that lead to the serious side effects when utilized in chemotherapy.

The current focus in the development of cancer therapies is on targeted drug delivery to provide therapeutic concentrations of anticancer agents at the site of action and spares the normal tissues.⁴ To date most reports describe the delivery of VBLS are through passive targeting. Marinina and colleagues have encapsulated two vinca alkaloids, vincristine sulfate and VBLS, in poly(lactide-co-glycolide), to obtain microspheres that can release the drugs in a sustained manner.³ Zhigaltseva and their research group have compared the drug-loading and retention properties of vincristine, vinorelbine and vinblastine when entrapped in liposomes.⁵ Dandamudi has incorporated VBLS into liposomes in combination with magnetic drug targeting, which showed ideal drug-loading efficiency.⁶

In this study, we have tried to overcome the side effects of VBLS by using folate-conjugated-bovine serum albumin nanoparticles (FA-BSANP)s as a targeting drug carrier system. Folate has attracted significant attention as a targeting moiety due to its high binding affinity, small size, low cost and that a folate receptor is expressed, in high levels, on the surface of many human cancers although in very low levels on normal tissues.^{7,8} Folate has also been reported having a pronounced effect on improving cellular uptake and the efficacy of anticancer drugs. Xue Han and colleagues have encapsulated 9-nitro-camptothecin (9-NC) into folate-conjugated polymer micelles (FA-M-9-NC) by mixing folate-polyethyleneglycol-distearoylphosphatidylethanolamine (folate-PEG-DSPE) and 1,2-Distearoyl-phosphatidyl ethanolamine-methylpolyethyleneglycol conjugate (MPEG-DSPE). *In vitro* drug efficacy against Hela cells showed increased cellular uptake for FA-M-9-NC than MPEG-DSPE-9-NC (M-9-NC) and free 9-NC. The killing ability of FA-M-9-NC against Hela cells was also significantly improved when compared with M-9-NC and free 9-NC.⁹ Prabakaran and colleagues have entrapped doxorubicin into folate-conjugated amphiphilic hyperbranched block copolymer (H40-PLA-b-MPEG/PEG-FA) micelles. Due to the folate-receptor-mediated endocytosis, both cellular uptake and cytotoxicity of doxorubicin-loaded H40-PLA-b-MPEG/PEG-FA against 4T1 mouse mammary carcinoma cell line were higher than doxorubicin-loaded H40-PLA-b-MPEG micelles.¹⁰ Moreover, folate was also identified as an active targeting moiety of the blood-brain barrier, and has already been reported as being effective in

targeting brain tumors.¹¹ Bellamkonda and colleagues have formulated a phospholipid-polyethylene glycol (PEG) mask to protect folate from reticuloendothelial system (RES) clearance, achieving a long-circulating targeting liposome for brain tumors. *In vivo* uptake studies, conducted with a 9L/lacZ glioma model, confirmed higher intracellular delivery of the obtained folate conjugated liposomes.¹²

The utilization of serum albumin as carriers for drug delivery is a part of ever growing pharmacological research. Lei Yang has entrapped 10-hydroxycamptothecin into bovine serum albumin nanoparticles (BSANP) to conquer its insolubility in water, and obtained nanoparticles with the mean particle size of 600 nm using a high-speed emulsification method.¹³ Feng-Qian Li and colleagues have prepared sodium ferulate loaded BSANPs using a desolvation procedure which passively targeted liver cells through the effects of particle sizes and surface characteristics.¹⁴ Karmali has targeted clinically approved paclitaxel-albumin nanoparticles to mice bearing human cancer xenografts by conjugating them with two tumor-homing peptides, CREKA (Cys-Arg-Glu-Lys-Ala) and LyP-1 (lysine permease), and the resulting targeted drug delivery systems were more effective than the unmodified ones.¹⁵ However, those studies only varied one factor at a time and as such their studies lack the representative effect of the interaction between different factors.¹⁶ Thus, we use a response surface methodology (RSM) for optimizing the process of producing BSANPs and studying the linear, square and interactive effects of various factors.

Therefore, we have focused on developing a FA-BSANPs targeting drug delivery system loaded with vinblastine sulfate (FA-BSANPs-VBLS), based on the optimized BSANPs preparation formulation that resulted from the RSM design. This system can passively target tumor cells passively through size effect and actively through folate, allowing a decreased drug dosage to reduce the undesirable side effects of VBLS. A freeze-drying process was adopted to obtain a dry powder form for long-term stability and preservation of the original pharmaceutical and biological properties of the products.¹⁷ Since freeze-drying was one of the major techniques in producing the FA-BSANPs-VBLS, mannitol was added as a lyoprotectant, and its effect on preventing FA-BSANPs-VBLS from aggregation after freeze-drying was demonstrated by scanning electron microscopy (SEM).

Materials and methods

Materials

Folate (FA), bovine serum albumin (BSA) trypsin and 2,4,6-trinitrobenzenesulfonic acid (TNBS) were all

obtained from Sigma Aldrich (St. Louis, MO, USA). The vinblastine sulfate was kindly provided by Hisun Pharmaceutical Co. Ltd (Zhejiang, China). N-hydroxysuccinimide, 1,3-dicyclohexylcarbodiimide (DCC), ethanol and the other reagents were all analytical grade.

Preparation and optimization of BSANPs by RSM

The BSANPs were prepared as previously described using a desolvation technique.¹⁸ As shown in Figure 1a, briefly, after BSA (3.21 mg) was first dissolved in deionized water (1 mL), a desolvating reagent, ethanol (4.23 mL), was added with a peristaltic pump TI/62/20 (Medorex, Norten-Hardenberg, Germany) (2.96 mL/min) at room temperature. Hereafter, glutaraldehyde solution (11.5 μ L, 0.25%) was added to

crosslink amino groups of the BSANPs. The crosslinking process was performed through stirring the suspension over a time period of 24 hours.

The desolvating reagent was removed by evaporation using a rotary evaporator R201BL (SENCO, Shanghai, China) at 40 °C, and then the BSANPs were redispersed to the original volume with deionized water. The redispersion process was performed in an ultrasonication bath TI-H-5 (Elma, Singen, Germany) over 10 minutes.

The above BSANPs preparation procedure was optimized by a four-factor, three-level central composite design (CCD), with BSA concentration (X_1), ethanol rate (X_2), ethanol amount (X_3) and theoretical crosslinking degree (X_4) as the independent variables (Table 1). The levels of those independent variables were based on preliminary trials.

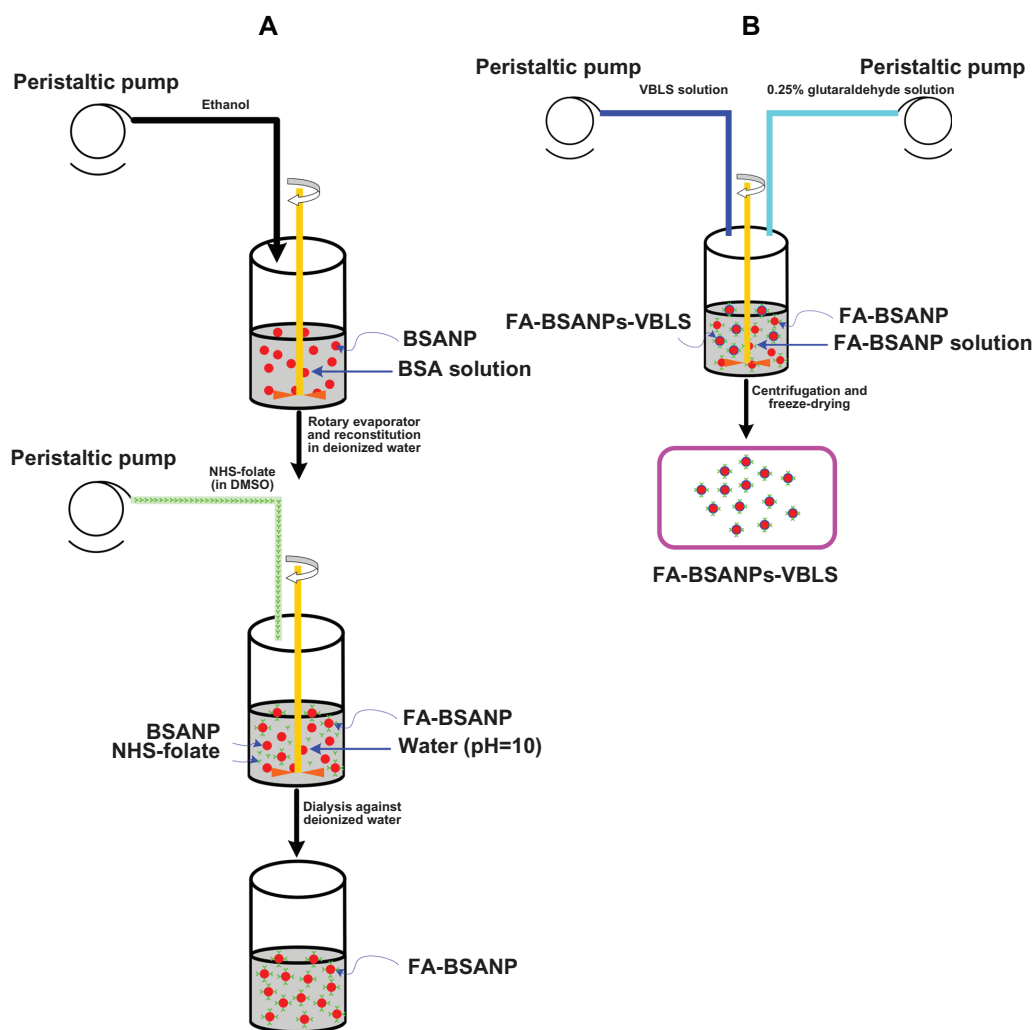


Figure 1 Schematic description of the preparation procedure of FA-BSANPs-VBLS **A**) BSANPs were produced with a desolvation technique, and then NHS-folate was conjugated under alkaline condition, pH = 10 **B**) FA-BSANP powder was reconstituted in deionized water, followed by the addition of VBLS solution with peristaltic pump. VBLS was loaded by means of electrostatic interaction.

Abbreviations: BSANP, bovine serum albumin nanoparticles; FA-BSANP, folate-conjugated-bovine serum albumin nanoparticles; FA-BSANPs-VBLS, folate-conjugated-bovine serum albumin nanoparticles-vinblastine sulfate; NHS-folate, N-Hydroxysuccinimide ester of folate; VBLS, vinblastine sulfate.

Table 1 Factors and their levels in RSM designs

Independent variables	Symbol	Coded levels		
		-1	0	1
BSA con.(mg/ml)	X_1	2	3	4
Ethanol rate (ml/min)	X_2	1.625	2.75	3.875
Ethanol amount (ml)	X_3	2.375	4.25	6.125
Degree of Crosslinking (%)	X_4	20	30	40

Abbreviations: BSA, bovine serum albumin; RSM, response surface methodology.

The mean particle size and residual amino groups of the resulting BSANPs were used as response variables. Design-Expert® Version 7.0.0 software (State-Ease Inc., Minneapolis, MN, USA) was applied to generating and evaluating the statistical experimental design.

Preparation of vinblastine sulfate-loaded folate-conjugated albumin nanoparticles

Preparation of FA-BSANPs

The method used for preparing the N-Hydroxysuccinimide ester of folate (NHS-folate) was reported by Lee and Low.¹⁹

The carboxylic groups of the NHS-folate were conjugated with the amino groups of the BSANPs under alkaline condition (pH 10.0). NHS-folate (3 mg) was dissolved in dimethyl sulfoxide (1.0 mL) and added to a BSANPs suspension stirring continuously (Figure 1a). The pH value of the BSA suspension was adjusted using 1M carbonate/bicarbonate buffer. This reaction took 45 min. Then the unassociated NHS-folate in the mixture was removed by dialyzing it against deionized water using Slide-A-Lyzer® dialysis cassettes with a molecular weight cut-off of 3500Da for 48 hours (Pierce Biotechnology, Rockford, IL, USA), followed by freeze-drying. The FA-BSANPs obtained after freeze-drying were a yellow powder.

Preparation of vinblastine sulfate-loaded FA-BSANPs

In the preliminary trials, we found that the produced drug carrier system would be unstable if VBLS was entrapped during the step when the BSANPs were formed. Thus a two-step preparation procedure was adopted, where the FA-BSANPs were used as porous drug carriers to some extent.²⁰ The VBLS was loaded mainly through electrostatic interaction between positive charges of the drug and negative charges of the FA-BSANPs, when the pH value of the solution was higher than the isoelectric point of BSA. This mechanism of loading

drugs has also been reported by Huang and colleagues.²¹ As illustrated in Figure 1b, the FA-BSANPs powder was reconstituted in deionized water, and then the VBLS solution was added into the resulting suspension. This mixture was stirred for 24 hours, allowing the VBLS to diffuse into the inner matrix of the FA-BSANPs. Thereafter, the mixture was freeze-dried followed by reconstitution in deionized water. In order to keep the VBLS in the FA-BSANPs matrix, glutaraldehyde solution (150 μ L, 0.25%) was added to the reconstitution solution to further crosslink the residual amino groups of the FA-BSANPs.

This reconstitution solution was centrifuged (20,000 \times g, 10 min) for the purpose of separating the unloaded VBLS. This purification process was repeated three times. After each centrifugation, the residue was redispersed, to the original volume, with deionized water, using a mechanical stirrer. The supernatant from each centrifugation was collected together to determine the drug entrapment efficiency and drug-loading efficiency. The resulting solution was freeze-dried again after final redispersion. The lyoprotectant, mannitol, would be added to the final redispersed solution (5% of total mass) before freeze-drying if needed.

Characterization of the FA-BSANPs-VBLS

Quantification of the residual amino groups on the BSANPs

The residual amino acid groups on the BSANPs were determined using trinitrobenzenesulphonic acid (TNBS) assay according to literature with minimum change.²²

The BSANPs were washed three times with water by centrifugation at 20,000 \times g for 20 min, followed by redispersion with 4% sodium bicarbonate solution (pH 8.5). Two milliliters of the BSANPs dispersion and 4.0 mL of TNBS solution (4.0 mol/mL in 4% sodium bicarbonate solution) were added. The reaction mixture was shaken at 400 rpm for one hour at 40 °C. The samples were again centrifuged (20,000 \times g; one hour) to separate the BSANPs from the supernatant. In order to measure any unreacted TNBS, 0.9 mL of the supernatant was added to 0.1 mL of an aqueous valine solution (40 mol/mL) and incubated at 40 °C in the dark for one hour. Following this 5 mL of HCl (0.5 mM/L) were added and the absorbance of solution was measured at 410 nm against a blank prepared, as described above, but containing 0.1 mL of trichloroacetic acid (1%) instead of the valine solution. The residual amino groups on the particle surface were calculated relative to a TNBS reference that was treated in the same manner as described above, using water instead of the BSANPs dispersion.

Determination of folate content associated with the BSANPs

The amount of NHS-folate that had been conjugated with BSANPs was evaluated using the method described by Zhang and colleagues.²³ Briefly, after dialysis against deionized water, the FA-BSANPs (1 mg in 10 mL deionized water) were digested by trypsin (50 µg/mg BSA). Then the resultant tryptic hydrolysis of the FA-BSANPs was scanned using a UV-spectrophotometer (268 nm to 450 nm) (SHIMADZU, Tokyo, Japan), using BSANPs and tryptic hydrolysis of BSANPs as controls. The extent of NHS-folate conjugated was determined relative to a NHS-folate reference: $y = 14.951x - 0.847$, $R^2 = 0.999$ (y : NHS-folate concentration, µg/mL; x : absorption). The content of the conjugated folate was the mean of triplicate experiments.

Mean particle size and surface morphology of nanoparticles

The mean particle size of obtained nanoparticles was determined by dynamic light scattering using Zetasizer (Malvern Instrument, Worcestershire, England) with angle detection at 90°. Each experimental preparation was conducted in triplicate, and the mean particle size was calculated.

The morphology of the samples was investigated using scanning electron microscopy (FEI Co., Eindhoven, Netherland).

Drug encapsulation efficiency and loading efficiency

The VBLS in the supernatant was examined by high performance liquid chromatography (HPLC). A Waters high performance liquid chromatograph (Waters Corporation, Milford, MA, USA), consisting of a Waters 600 Controller equipped with a Waters 717 plus autosampler, and a Waters 2487 UV detector. The samples were chromatographed at 25 °C by injecting of 10 µL of sample into a Diamonsil C₁₈ column, (250 mm × 4.6 mm, 5 µm; Dikma Technologies, Beijing, China). The mobile phase was composed of an aqueous solution of ammonium carbonate (0.5%) and methanol 70:30 (v/v). The wavelength was set to 215 nm. The drug entrapment efficiency (DEE) and drug-loading efficiency (DLE) were calculated using equations as previously reported by Park and colleagues.⁷

$${}^1\text{DEE} = \frac{\text{VBLS (total)} - \text{VBLS(in supernatant)}}{\text{VBLS (total)}} \times 100\% \quad (1)$$

$${}^2\text{DLE} = \frac{\text{VBLS (total)} - \text{VBLS (in supernatant)}}{\text{FA - BSANPs} - \text{VBLS}} \times 100\% \quad (2)$$

Drug release study

VBLS release from FA-BSANPs was determined in phosphate buffered saline (0.15 M, pH 7.4) at 37 °C. FA-BSANPs-VBLS suspension (5.8 mg/mL, 10 mL; without mannitol) was placed in Slide-A-Lyzer® dialysis cassettes (MWCO 3500), and then the dialysis cassettes was immersed in a 400 mL beaker containing 200 mL release buffer. The beaker was then placed in an incubator shaker at 37 °C and 100 rpm. The release buffer (3 mL) was withdrawn from the beaker and replaced with 3 mL fresh release buffer at predetermined time intervals. The VBLS concentration in each collected release buffer sample was determined by HPLC using conditions as described above. The accumulative release percentage was calculated using the following equations:

$$C'_i = C_1$$

$$C'_{i+1} = C_{i+1} - \frac{(V - V_i)C_i}{V} \quad (3)$$

$$Q_i = \frac{\sum_{i=1}^i C'_i V}{M} \times 100\% \quad (4)$$

where C_i represents the VBLS concentration of each sample withdrawn at predetermined time intervals, C'_i represents the increase of the VBLS concentration during each time interval, V represents the volume of the release buffer, V_0 represents the volume of each withdrawn sample, M is the VBLS loaded in the FA-BSANPs-VBLS, and Q_i is the accumulative release percentage at predetermined time point.

The drug release studies were carried out in triplicate for each of the samples.

Results and discussion

Model analysis

Particle size plays a key role in determining body distribution of the nanoparticles after being injected *in vivo* and in facilitating their access into cancer cells after the folate has targeted cancer tissues. In order to investigate the mechanism determining the mean particle size of the BSANPs, we studied the linear, square, and interactive effects of the independent variables on particle size using RSM. On the other hand, the degree of crosslinking could influence the matrix structure of the BSANPs and therefore influence its drug

carrying capacity – since VBLS diffuses into the BSANPs mainly through channels within the matrix of the BSANPs. The degree of crosslinking can be controlled by adjusting the amount of glutaraldehyde. However, the association of folate with BSANPs is through conjugating the amino groups of BSA molecules with the carboxylic groups of the folate. Thus, the largest amount of the glutaraldehyde we added can only theoretically crosslink 50% of the overall amino groups of BSA molecules, leaving room for the folate conjugation.²⁴ This model was used to minimize the particle size while maximize the amino groups left on the surface of the BSANPs.

For the response surface methodology involving CCD, a total of 30 experiments were conducted for four factors at three levels. The uncoded independent variables and the observed responses for the 30 experiments are shown in Table 2. A suitable polynomial equation involving the main individual effects and interaction factors was selected based on the estimation of several statistical parameters, such as the multiple correlation coefficient (R^2), adjusted multiple correlation coefficient (adjusted R^2) and the predicted residual sum of squares (PRESS), provided by the Design-Expert[®] software. The smaller the PRESS statistic is, the better the model fits to the data point.²⁵ As shown in Table 3, due to their smallest value of PRESS, two quadratic models were chosen as a suitable statistical model for the optimization of the mean particle size and residual amino groups, respectively. The lack of fit of both models was statistically insignificant, as shown in Table 3. The models of each of the response variables generated by the design are given in the following equations.

$$\begin{aligned} \text{Mean particle size} = & 122.88 + 26.25X_1 + 13.06X_2 + 0.33X_3 \\ & - 5.30X_4 + 11.81X_1X_2 - 1.17X_1X_3 \\ & - 4.21X_1X_4 + 1.83X_2X_3 - 3.08X_2X_4 \\ & + 2.37X_3X_4 + 30.11X_1^2 + 9.84X_2^2 \\ & + 5.92X_3^2 + 10.41X_4^2 \end{aligned} \quad (5)$$

$$\begin{aligned} \text{Residual amino groups} = & 671.94 - 10.71X_1 + 2.95X_2 \\ & - 0.011X_3 - 20.52X_4 - 5.09X_1X_2 \\ & + 0.22X_1X_3 + 9.70X_1X_4 + 0.15X_2X_3 \\ & - 4.73X_2X_4 - 0.1X_3X_4 - 110.03X_1^2 \\ & - 105.19X_2^2 - 104.78X_3^2 - 6.51X_4^2 \end{aligned} \quad (6)$$

Analysis of variance (ANOVA) was applied to determine the significance and the magnitude of the effects of the main variables and their interactions on the response variables (Table 4). The regression models obtained were used to

Table 2 Experimental design and results of the central composite design

Assay	Variables				Responses	
	X_1	X_2	X_3	X_4	Y_1 (nm)	Y_2 (nmol/mg)
1	4	1.625	6.125	20	187.6	345.813
2	4	3.875	2.375	20	264.6	342.91
3	4	3.875	2.375	40	215.1	323.377
4	4	1.625	2.375	40	174.9	324.485
5	5	2.75	4.25	30	282.2	210.546
6	4	1.625	2.375	20	193.2	346.226
7	3	2.75	0.5	30	136.7	253.779
8	2	3.875	6.125	20	178.2	404.353
9	3	2.75	4.25	30	125.9	678.07
10	2	3.875	2.375	20	167.9	405.421
11	3	2.75	4.25	30	93.0	674.001
12	2	3.875	6.125	40	166.5	325.355
13	3	2.75	4.25	30	113.8	671.627
14	2	3.875	2.375	40	158.0	325.593
15	3	2.75	4.25	30	139.4	670.796
16	4	1.625	6.125	40	175.3	324.168
17	2	1.625	6.125	20	158.2	366.464
18	4	3.875	6.125	40	238.2	323.332
19	1	2.75	4.25	30	173.0	254.491
20	3	2.75	4.25	30	138.2	670.558
21	4	3.875	6.125	20	253.0	345.83
22	3	0.5	4.25	30	140.9	251.939
23	3	2.75	4.25	10	150.0	688.202
24	2	1.625	2.375	20	154.6	366.701
25	2	1.625	6.125	40	154.7	325.751
26	2	1.625	2.375	40	152.1	325.553
27	3	5	4.25	30	152.2	251.82
28	3	2.75	4.25	30	127.0	666.558
29	3	2.75	8	30	125.0	253.245
30	3	2.75	4.25	50	147.6	604.978

Abbreviations: BSA concentration (X_1), ethanol rate (X_2), ethanol amount (X_3) and theoretical crosslinking degree (X_4).
Particle size Y_1 , residual amino groups, Y_2 .

generate the three-dimensional response surface plots for the independent variables. According to the ANOVA, the BSA concentration and the rate of adding ethanol have significant effects on the particle size. Therefore, these variables were chosen to plot the response surface for the particle size while holding amount of ethanol and crosslinking degree at central points, 4.25 mL and 30%, respectively. As can be seen from Figure 2, the particle size increases markedly as the BSA concentration increases. The particle size had a slight decrease as the rate of adding ethanol is increased up to 2.75 mL/min, over this rate, the particle size had a minor increase when the rate of adding ethanol was increased. There is a more

Table 3 ANOVA for the models predicted for each response

Source	Y_1					Y_2				
	SS	DF	MS	F-value	P-value	SS	DF	MS	F-value	P-value
Model	50701.321	14	3621.523	8.522	<0.0001	768343.274	14	54881.662	1430.314	<0.0001
X_1	16542.75	1	16542.75	38.926	<0.0001	2750.79	1	2750.79	71.69	<0.0001
X_2	4095.094	1	4095.094	9.636	0.007	208.7	1	208.67	5.439	0.034
X_3	2.60	1	2.60	0.006	0.939	0.003	1	0.00299	0.0000778	0.993
X_4	675.220	1	675.220	1.589	0.227	10108.715	1	10108.715	263.451	<0.0001
X_1X_2	2230.201	1	2230.201	5.248	0.037	415.121	1	415.121	10.819	0.005
X_1X_3	21.856	1	21.856	0.051	0.824	0.762	1	0.762	0.0199	0.89
X_1X_4	283.081	1	283.081	0.666	0.428	1506.761	1	1506.761	39.269	<0.0001
X_2X_3	53.656	1	53.656	0.126	0.727	0.342	1	0.342	0.0089	0.926
X_2X_4	151.906	1	151.906	0.357	0.559	357.317	1	357.317	9.312	0.0081
X_3X_4	89.776	1	89.776	0.211	0.652	0.161	1	0.161	0.0042	0.949
X_1^2	24859.161	1	24859.161	58.495	<0.0001	332053.086	1	332053.086	8653.895	<0.0001
X_2^2	2657.250	1	2657.250	6.253	0.025	303480.724	1	303480.724	7909.248	<0.0001
X_3^2	960.529	1	960.529	2.26	0.154	301130.481	1	301130.481	7847.997	<0.0001
X_4^2	2969.646	1	2969.646	6.988	0.018	1162.392	1	1162.392	30.294	<0.0001
Residual	6374.679	15	424.979			575.555	15	38.37		
LOF ^a	4865.711	10	486.571	1.612	0.312	501.456	10	50.146	3.384	0.095
Pure Error	1508.968	5	301.794			74.099	5	14.82		
Cor Total	57076	29				768918.83	29			

^aLOF = lack of fit.

Abbreviations: BSA concentration (X_1), ethanol rate (X_2), ethanol amount (X_3) and theoretical crosslinking degree (X_4). Particle size Y_1 , residual amino groups, Y_2 .

pronounced effect with alterations in the BSA concentration, which can be foreseen from the ANOVA, since the P value of the BSA concentration is less than 0.0001.

According to the ANOVA, the BSA concentration and degree of crosslinking had pronounced effects on the residual amino groups. As shown in Figure 3a, when the amount of ethanol and crosslinking degree were held at center point, namely 4.25 mL and 30%, the residual amino groups have a maximal value as the BSA concentration and ethanol rate arrive at 3 mg/mL and 2.75 mL/min, respectively. Figure 3b indicate that the residual amino groups decreases as the crosslinking degree increases. Due to the interaction between the degree of crosslinking and the BSA concentration, the residual amino groups achieved a peak

value of 661.386 nM/mg when the BSA concentration and degree of crosslinking were approximately 3 mg/mL and 35%, respectively. As to the interaction between the rate of ethanol added and degree of crosslinking (Figure 3c), the same pattern was observed. In this case, the optimal value of the residual amino groups was 661.38 nM/mg. Theoretically, the degree of crosslinking should be the only parameter that has significant effect on the residual amino groups.²⁴ However, the observed results may be due to the fact that the residual amino groups on the BSANPs are also influenced by the particle size, since the smaller the particle is, the larger the relative surface area, thus there are more amino groups exposed on the surface of the nanoparticles. In another word, the two variables that had significant effects

Table 4 Optimization formulation of the BSANPs and the predicted and observed responses

Factors				Predicted responses		Observed responses		Predicted error ^c	
X_1	X_2	X_3	X_4	Y_1	Y_2	$Y_1 \pm SD^b$	$Y_2 \pm SD^b$	Y_1	Y_2
3.21	2.96	4.23	20	150 nm	674.598 nmol/mg	156.6 \pm 3.8	668.973 \pm 27.5	-4.427%	0.834%

^bn = 5.

^cPredicted error (%) = (predicted value – observed value)/predicted value \times 100%.

Abbreviation: BSANP, bovine serum albumin nanoparticles.

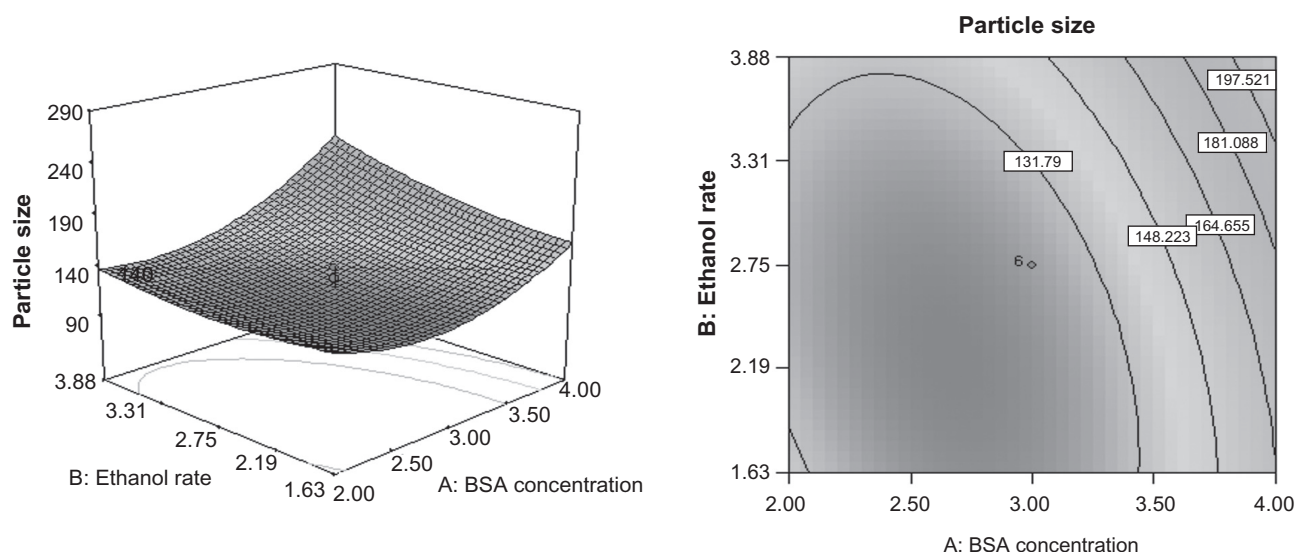


Figure 2 Response surface plots for mean particle size of the BSANPs showing interaction between BSA concentration and ethanol rate.
Abbreviations: BSANP, bovine serum albumin nanoparticles; BSA, bovine serum albumin.

on particle size interacted with the fourth variables, the degree of crosslinking, resulting in the data obtained.

Nanoparticles with the mean particle size of 100 to 200 nm have an enhanced permeability and retention (EPR) effect, which allowed the preferred accumulation of drug-loaded nanoparticles within tumors.²⁶ Moreover, pegylated liposomes with the mean particle size of 120 to 160 nm were found to circulate in blood for long periods of time.²⁷ Hence, 150 nm was chosen as the target for the optimization of the mean particle size of the BSANPs, while maximization was the chosen aim of the optimization for the residual amino groups. The optimum values of the variables were obtained by graphical and numerical analyses using the Design-Expert[®] software and based on the criterion of desirability.²⁵ The optimized formulation was achieved with 3.21 mg/mL BSA, 2.96 mL/min of ethanol rate, 4.23 mL ethanol, and 20% crosslinking degree. The desirability of this formulation is 0.986. Thus, five new batches of the BSANPs were prepared to confirm the validity of the optimization procedure. Table 4 indicates a predicted error of -4.427% for mean particle size and a predicted error of 0.834% for residual amino groups, respectively. Thereafter, all of the following experiments were conducted using BSANPs produced by this optimized formulation.

Characterization of the nanoparticles

Determination of the conjugation of folate to BSANPs
 NHS-folate had an absorption maximum at 281 nm, the absorption peak of digested FA-BSANPs at 281 nm

confirmed the successful conjugation of folate with BSANPs (Figure 4). Moreover, according to the calibration curve of NHS-folate, 383.996 μ M NHS-folate was conjugated with 1 g of BSANPs, which was rather high compared with traditional procedures of preparing the BSANPs.²² On one hand, this phenomenon indicates that the amino groups of the BSA molecules were consumed when superfluous glutaraldehyde was added to crosslink BSANPs in the traditional procedures. On the other hand, it verifies our postulation that the residual amino groups can be adjusted when the crosslinking agent was added stoichiometrically.

Drug entrapment and loading efficiency

We investigated the influence of different particle size of the FA-BSANPs and varying the initial weight ratio of the VBLS to the FA-BSANPs on the drug entrapment efficiency and the drug-loading efficiency. The NO.11, NO.23 and the optimized formulation designed by response surface methodology were used in this part, considering the mean particle size of the resulting BSANPs (93, 156.6, and 282.2 nm). As can be seen from Figure 5, the larger the nanoparticles are, the higher the drug entrapment efficiency, as well as the drug-loading efficiency. This may result from the fact that larger FA-BSANPs have a larger volume, thus can hold more drugs. The highest drug entrapment efficiency and drug-loading efficiency were obtained, (namely 94.78% and 47.66%), when the FA-BSANPs had an average diameter of 282.2 nm. On the other hand, in each group with different diameters, the drug entrapment efficiency and the drug-loading efficiency

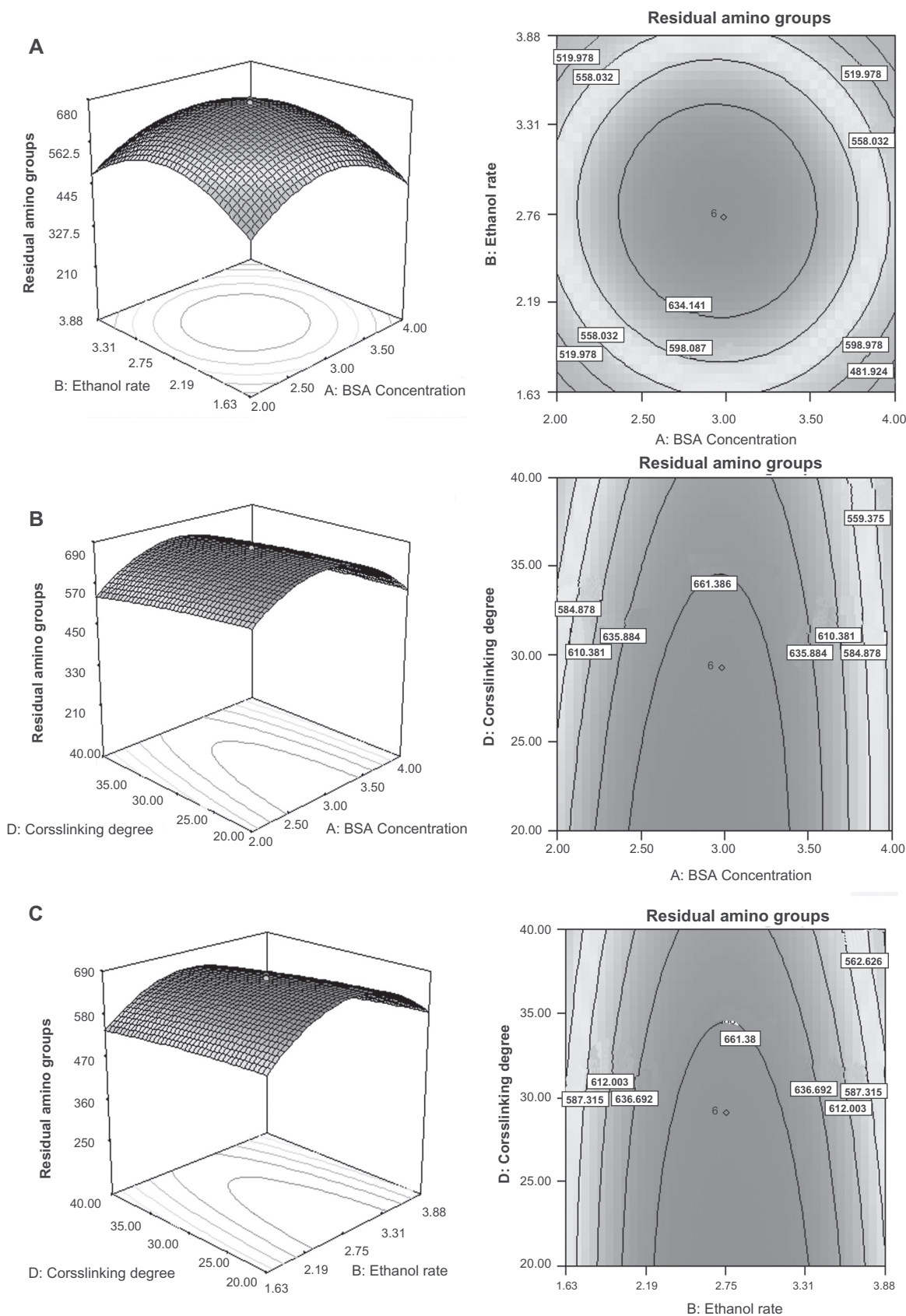


Figure 3 Residual amino groups of the BSNPs showing interaction between **A)** BSA concentration and ethanol rate; **B)** BSA concentration and crosslinking degree; **C)** ethanol rate and crosslinking degree.
Abbreviations: BSNP, bovine serum albumin nanoparticles; BSA, bovine serum albumin.

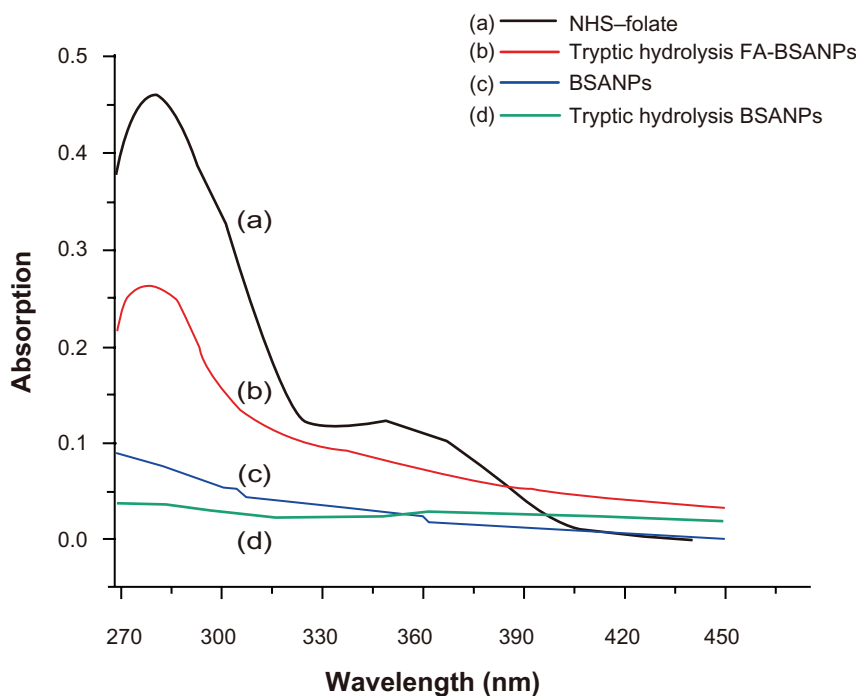


Figure 4 Determination of NHS-folate conjugation with BSANPs. **A)** NHS-folate has two absorption peaks, namely 281 nm and 345 nm. **B)** Tryptic hydrolysis FA-BSANPs has absorption at 281 nm, and the unassociated NHS-folate has been removed by dialysis. **C)** and **D)** BSANPs and tryptic hydrolysis have no effect on NHS-folate absorption. **Abbreviations:** BSANP, bovine serum albumin nanoparticles; FA-BSANP, folate-conjugated-bovine serum albumin nanoparticles; NHS-folate, N-Hydroxysuccinimide ester of folate.

increased as the initial weight ratio of VBLS to BSA increased from 1:6 to 1:2, which indicates there are maximal carrying capacities for the FA-BSANPs.

Despite the high drug entrapment efficiency and drug-loading efficiency of NO.5, the mean particle size and the resulting characteristics are still the priority of

preparing the tumor-specific drug carrier. Moreover, the drug entrapment efficiency and the drug-loading efficiency of the optimized formulation were acceptable for drug delivery system.²⁸ Thus, the FA-BSANPs-VBLS prepared with the optimized formulation were used in the drug release study *in vitro*.

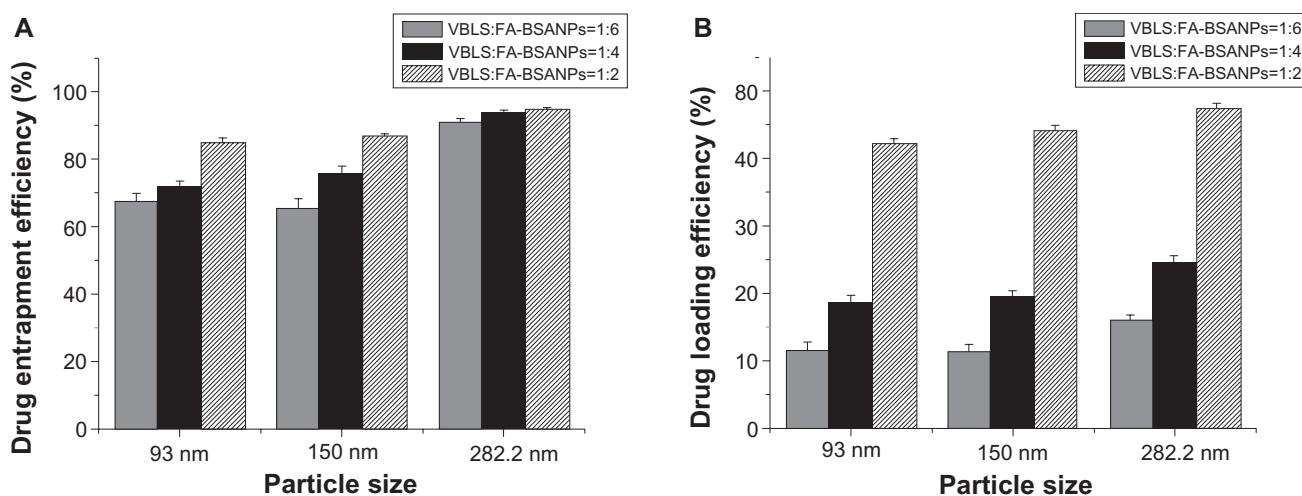


Figure 5 Investigation of the influence of particle size and weight ratio between VBLS and FA-BSANPs on **A)** drug entrapment efficiency and **B)** drug-loading efficiency of FA-BSANPs-VBLS ($\bar{X} \pm SD$, $n = 3$).

Abbreviations: FA-BSANP, folate-conjugated-bovine serum albumin nanoparticles; FA-BSANPs-VBLS, folate-conjugated-bovine serum albumin nanoparticles-vinblastine sulfate; VBLS, vinblastine sulfate.

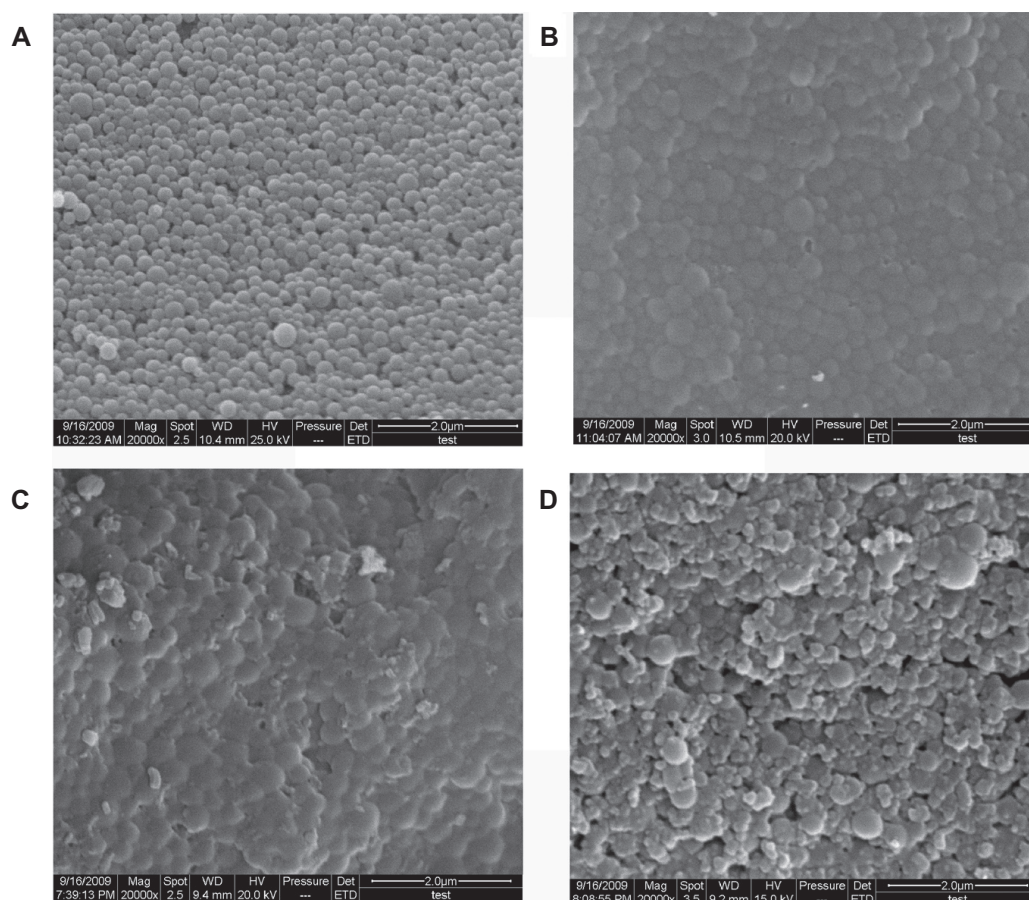


Figure 6 Comparison of SEM images of nanoparticles obtained in the steps of producing the optimal formulation of folate-conjugated-bovine serum albumin nanoparticles-vinblastine sulfate (FA-BSANPs-VBLS): **A**) bovine serum albumin nanoparticles (BSANPs); **B**) folate-conjugated-bovine serum albumin nanoparticles (FA-BSANPs); **C**) FA-BSANPs-VBLS; **D**) FA-BSANPs-VBLS with mannitol.

Abbreviations: BSANP, bovine serum albumin nanoparticles; FA-BSANP, folate-conjugated-bovine serum albumin nanoparticles; FA-BSANPs-VBLS, folate-conjugated-bovine serum albumin nanoparticles- vinblastine sulfate; NHS-folate, N-Hydroxysuccinimide ester of folate; VBLS, vinblastine sulfate; SEM, scanning electron microscopy.

Surface characteristics of BSANPs

In order to examine and compare the surface characteristics of the nanoparticles resulting from each step in preparing the optimal formulation of FA-BSANPs-VBLS, they were prepared and scanned using SEM. As shown in Figure 6, all of the nanoparticles were globular-shaped. The blank BSANPs were evenly distributed in particle size and had a tight structure, while the conjugation of the folate with the BSANPs changed the surface characteristics of BSANPs, and led to agglomeration to some extent (Figure 6b). The adjustment of pH value to alkaline conditions (pH = 10) before conjugating the folate may account for this phenomenon, since the pH value also plays a significant role in stabilizing the nanoparticles.²⁹ However, the addition of mannitol in the final products can solve this problem, as can be seen in Figure 6d, since the aggregation still existed after VBLS was loaded into FA-BSANPs (Figure 6c). The FA-BSANPs-VBLS were well dispersed after adding mannitol. Moreover, no crystal precipitations were



Figure 7 Appearance of FA-BSANPs-VBLS solution, 48 hours after reconstitution. **Abbreviation:** FA-BSANPs-VBLS, folate-conjugated-bovine serum albumin nanoparticles-vinblastine sulfate.

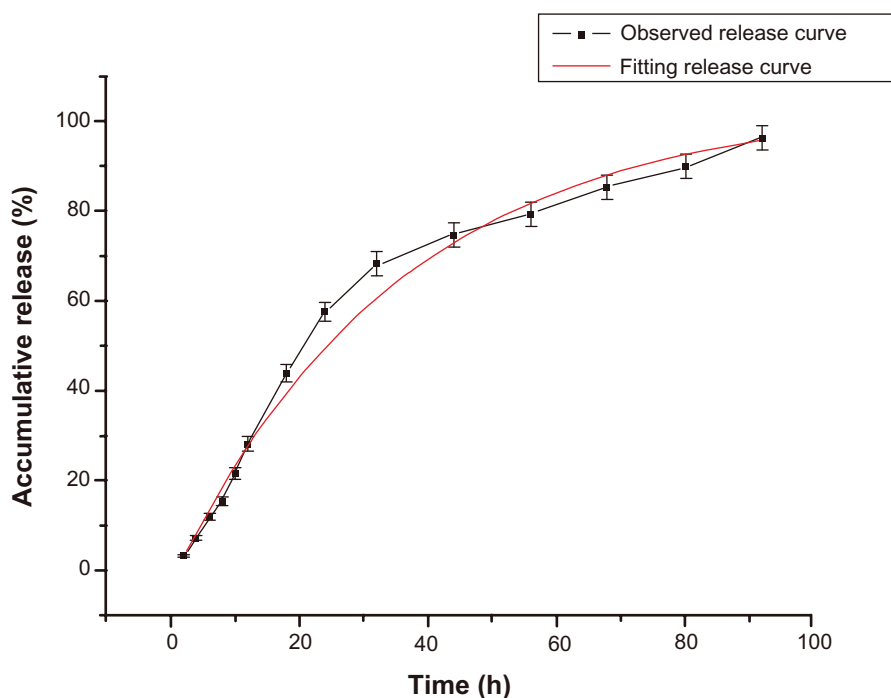


Figure 8 FA-BSANPs-VBLS accumulative drug release profile and its fitting curve of first order kinetics model. Data shows $\bar{X} \pm SD$ ($n = 3$).
Abbreviations: FA-BSANPs-VBLS, folate-conjugated-bovine serum albumin nanoparticles-vinblastine sulfate.

observed in FA-BSANPs-VBLS, and FA-BSANPs-VBLS with mannitol, which demonstrates the stability and applicability of the obtained drug delivery system.

Drug release property of the drug carrier system

The FA-BSANPs-VBLS powder without mannitol was reconstituted to carry out *in vitro* drug release experiments. The appearance of the reconstitution solution was translucent, tainted with light yellow color after being reconstituted for 48 hours (Figure 7).

The batch used to conduct the drug release experiment had an average drug entrapment efficiency of 88.06% and an average drug-loading efficiency of 39.14%, respectively (in triplicate). The drug carrier system had a burst release in 12 hours and a slow release up to 56 hours, releasing approximately 30% and 80% of VBLS respectively (Figure 8). The observed release curve indicates that the drug carrier system had a sustained release property. Moreover, the observed release curve was analysed using the Originpro (Version 7.5) software (OriginLab Corporation, Northampton, USA). The observed release model was in close agreement with the first order kinetics model, as shown in Figure 8, with R^2 of 0.991 and equation of $y = -106.451 e^{(-x/35.151)} + 103.386$. The fitting of the first order kinetics model confirmed the sustained release feature of this drug delivery system.

Conclusions

The RSM has been successfully applied to optimize the procedure for the preparation of BSANPs. Our results indicated that the BSA concentration and the ethanol addition rate played significant roles in determining the BSANPs particle size, and it is mainly through these interactive effects that the four independent variables affected the amount of residual amino groups on the surface of the BSANPs. The VBLS entrapment and loading efficiency were investigated, and extra considerations were paid to the influence of the particle sizes on the drug entrapment efficiency and drug-loading efficiency. Both drug entrapment efficiency and drug-loading efficiency were improved with increased particle size, as well as an increased VBLS to BSA ratio. The surface characterization demonstrated that the FA-BSANPs-VBLS with mannitol was a suitable drug delivery system, and the *in vitro* release study verified its sustained release characteristics. Furthermore, the *in vivo* properties of the FA-BSANPs-VBLS targeting drug delivery system will be investigated in the future.

Acknowledgments

The authors appreciate the comments and careful corrections made by anonymous reviewers. The project was supported by the National Key Technology Research and Development Program (2006BAD18B0401), National

Natural Science Foundation of China (No.30600052), Program for New Century Excellent Talents in University NCET-06-0329, Young Science Foundation of Heilongjiang Province QC08C30, and Program of Science and Technology from State Forestry Administration (2007–12). The authors also express their gratitude to Yongzhi Cui for conducting SEM analysis.

References

- Cragg GM, Newman DJ. Plants as a source of anti-cancer agents. *J Ethnopharmacol.* 2005;100(1–2):72–79.
- Kruczynski A, Barret JM, Etievant C, et al. Antimitotic and tubulin-interacting properties of vinflunine, a novel fluorinated vinca alkaloid. *Biochem Pharmacol.* 1998;55(5):635–648.
- Marinina J, Shenderova A, Mallery S, Schwendeman S. Stabilization of vinca alkaloids encapsulated in poly(lactide-co-glycolide) microspheres. *Pharm Res.* 2000;17(6):677–683.
- Jain KK. targeted drug delivery for cancer. *Technol Cancer Res Treat.* 2005;4(4):3.
- Zhigaltsev IV, Maurer N, Akhong QF, et al. Liposome-encapsulated vincristine, vinblastine and vinorelbine: a comparative study of drug loading and retention. *J Control Release.* 2005;104(1):103–111.
- Dandamudi S, Campbell RB. The drug loading, cytotoxicity and tumor vascular targeting characteristics of magnetite in magnetic drug targeting. *Biomaterials.* 2007;28(31):4673–4683.
- Park EK, Lee SB, Lee YM. Preparation and characterization of methoxy poly(ethylene glycol)/poly(epsilon-caprolactone) amphiphilic block copolymeric nanospheres for tumor-specific folate-mediated targeting of anticancer drugs. *Biomaterials.* 2005;26(9):1053–1061.
- Park EK, Kim SY, Lee SB, Lee YM. Folate-conjugated methoxy poly(ethylene glycol)/poly([var epsilon]-caprolactone) amphiphilic block copolymeric micelles for tumor-targeted drug delivery. *J Control Release.* 2005;109(1–3):158–168.
- Han X, Liu J, Liu M, et al. 9-NC-loaded folate-conjugated polymer micelles as tumor targeted drug delivery system: preparation and evaluation in vitro. *Int J Pharm.* 2009;372(1–2):125–131.
- Prabaharan M, Grailler JJ, Pilla S, Steeber DA, Gong S. Folate-conjugated amphiphilic hyperbranched block copolymers based on Boltorn H40, poly(L-lactide) and poly(ethylene glycol) for tumor-targeted drug delivery. *Biomaterials.* 2009;30(16):3009–3019.
- Beduneau A, Saulnier P, Benoit JP. Active targeting of brain tumors using nanocarriers. *Biomaterials.* 2007;28(33):4947–4967.
- McNeeley KM, Karathanasis E, Annapragada AV, Bellamkonda RV. Masking and triggered unmasking of targeting ligands on nanocarriers to improve drug delivery to brain tumors. *Biomaterials.* 2009;30(23–24):3986–3995.
- Yang L, Cui F, Cun D, Tao A, Shi K, Lin W. Preparation, characterization and biodistribution of the lactone form of 10-hydroxycamptothecin (HCPT)-loaded bovine serum albumin (BSA) nanoparticles. *Int J Pharm.* 2007;340(1–2):163–172.
- Li FQ, Su H, Wang J, et al. Preparation and characterization of sodium ferulate entrapped bovine serum albumin nanoparticles for liver targeting. *Int J Pharm.* 2008;349(1–2):274–282.
- Karmali PP, Kotamraju VR, Kastantin M, et al. Targeting of albumin-embedded paclitaxel nanoparticles to tumors. *Nanomedicine.* 2009;5(1):73–82.
- Preetha B, Viruthagiri T. Application of response surface methodology for the biosorption of copper using *Rhizopus arrhizus*. *J Hazard Mater.* 2007;143(1–2):506–510.
- Oh KT, Lee ES, Kim D, Bae YH. L-histidine-based pH-sensitive anti-cancer drug carrier micelle: reconstitution and brief evaluation of its systemic toxicity. *Int J Pharm.* 2008;358(1–2):177–183.
- Weber C, Kreuter J, Langer K. Desolvation process and surface characteristics of HSA-nanoparticles. *Int J Pharm.* 2000;196(2):197–200.
- Lee R, Low P. Delivery of liposomes into cultured KB cells via folate receptor-mediated endocytosis. *J Biol Chem.* 1994;269(5):3198–3204.
- Sher P, Ingavle G, Ponrathnam S, Pawar AP. Low density porous carrier drug adsorption and release study by response surface methodology using different solvents. *Int J Pharm.* 2007;331(1):72–83.
- Huang SJ, Sun SL, Feng TH, Sung KH, Lui WL, Wang LF. Folate-mediated chondroitin sulfate-Pluronic 127 nanogels as a drug carrier. *Eur J Pharm Sci.* 2009;38(1):64–73.
- Zhang L, Hou S, Mao S, Wei D, Song X, Lu Y. Uptake of folate-conjugated albumin nanoparticles to the SKOV3 cells. *Int J Pharm.* 2004;287(1–2):155–162.
- Zhang L, Hou S, Mao S, Wei D, Song X, Lu Y. Uptake of folate-conjugated albumin nanoparticles to the SKOV3 cells. *Int J Pharm.* 2004;287(1–2):155–162.
- Langer K, Anhorn MG, Steinhauser I, et al. Human serum albumin (HSA) nanoparticles: Reproducibility of preparation process and kinetics of enzymatic degradation. *Int J Pharm.* 2008;347(1–2):109–117.
- Kim MS, Kim JS, You YH, et al. Development and optimization of a novel oral controlled delivery system for tamsulosin hydrochloride using response surface methodology. *Int J Pharm.* 2007;341(1–2):97–104.
- Maeda H, Wu J, Sawa T, Matsumura Y, Hori K. Tumor vascular permeability and the EPR effect in macromolecular therapeutics: a review. *J Control Release.* 2000;65(1–2):271–284.
- Momekova D, Rangelov S, Yanev S, et al. Long-circulating, pH-sensitive liposomes sterically stabilized by copolymers bearing short blocks of lipid-mimetic units. *Eur J Pharm Sci.* 2007;32(4–5):308–317.
- Li X, Jasti BR. *Design of Controlled Release Drug Delivery Systems*. New York, NY: McGraw-Hill; 2006.
- Langer K, Balthasar S, Vogel V, Dinauer N, von Briesen H, Schubert D. Optimization of the preparation process for human serum albumin (HSA) nanoparticles. *Int J Pharm.* 2003;257(1–2):169–180.

International Journal of Nanomedicine

Publish your work in this journal

The International Journal of Nanomedicine is an international, peer-reviewed journal focusing on the application of nanotechnology in diagnostics, therapeutics, and drug delivery systems throughout the biomedical field. This journal is indexed on PubMed Central, MedLine, CAS, SciSearch®, Current Contents®/Clinical Medicine,

Submit your manuscript here: <http://www.dovepress.com/international-journal-of-nanomedicine-journal>

Dovepress

Journal Citation Reports/Science Edition, EMBASE, Scopus and the Elsevier Bibliographic databases. The manuscript management system is completely online and includes a very quick and fair peer-review system, which is all easy to use. Visit <http://www.dovepress.com/testimonials.php> to read real quotes from published authors.